

Supplementary Information

Modeling Tetracycline Adsorption onto Blast Furnace Slag Using Statistical and Machine Learning Approaches

Harsha S. Rangappa ^{1,2}, Phyū Phyū Mon ³, Indika Herath ⁴, Giridhar Madras ⁵, Chuxia Lin ² and Challapalli Subrahmanyam ^{1,3,*}

¹ Center for Interdisciplinary Programs, Indian Institute of Technology Hyderabad, Kandi, Sangareddy 502285, India

² Centre for Regional and Rural Futures, Faculty of Science, Engineering and Built Environment, Deakin University, Burwood, VIC 3125, Australia

³ Department of Chemistry, Indian Institute of Technology Hyderabad, Kandi, Sangareddy 502285, India

⁴ Centre for Regional and Rural Futures, Faculty of Science, Engineering and Built Environment, Deakin University, Waurn Ponds, VIC 3216, Australia

⁵ Department of Chemical Engineering, Indian Institute of Technology Hyderabad, Kandi, Sangareddy 502285, India

* Correspondence: csubbu@iith.ac.in

Number of pages: 11

Number of figures: 9

Number of tables: 6

Figures:

Figure.S1. (a) Artificial Neural Network architecture for modeling the adsorption of TC into GGBS-Ox (b) Random Forest architecture for modeling the adsorption of TC into GGBS-Ox

Figure. S2. N₂ adsorption and desorption isotherms of GGBS and GGBS-Ox

Figure. S3. N₂ adsorption/desorption curves of different adsorbents (insert: pore size distribution). (Page S10).

Figure. S3. (a) Particle size distribution by dynamic light scattering (DLS) of GGBS (b) Particle size distribution by dynamic light scattering (DLS) of GGBS-Ox

Figure. S4. (a)The effect of adsorbent dosage on percentage removal (b) the effect of pollutant concentration on the percentage removal.

Figure. S5. (a) Comparison of predicted and actual results for RSM (b) Comparison of predicted and actual results for ANN (c) Comparison of predicted and actual results for RF

Figure. S6. Perturbation plot for TC removal efficiency.

Figure. S7. Kinetics of adsorption of TC (a) First-order kinetics (b) Second-order kinetics.

Figure. S8. Effect of the temperature on the adsorption capacity of TC by GGBS-Ox.

Fig. S9. Thermodynamic parameters of TC adsorption by GGBS-Ox.

Tables:

Table S1. Levels of parameters for BBD experiments.

Table S2. Comparison of RSM, ANN, and RF

Table S3. Calculation of adsorption parameters and regression coefficients

Table S4. The parameters and regression coefficients for pseudo-first order and pseudo-second order are listed below.

Table S5: The parameters and regression coefficients for Langmuir, Freundlich, DR isotherm and McKay external diffusion model

Table S6. Thermodynamic conditions for GGBS-Ox adsorption at different temperatures.

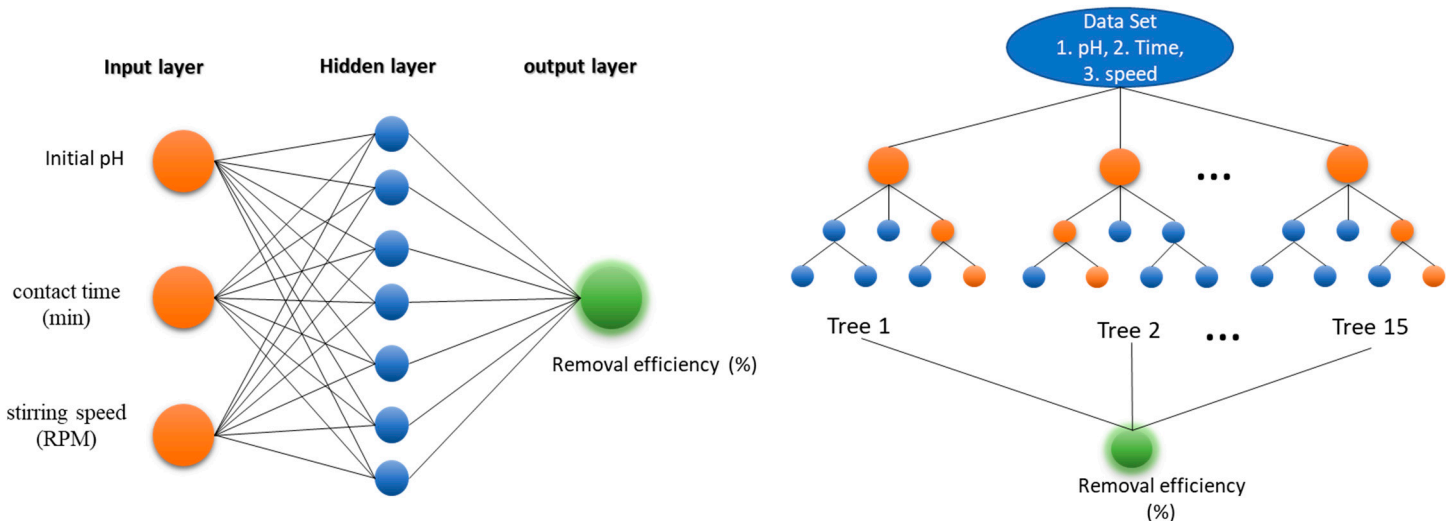


Figure. S1. (a) Artificial Neural Network architecture for modeling the adsorption of TC into GGBS-Ox (b) Random Forest architecture for modeling the adsorption of TC into GGBS-Ox

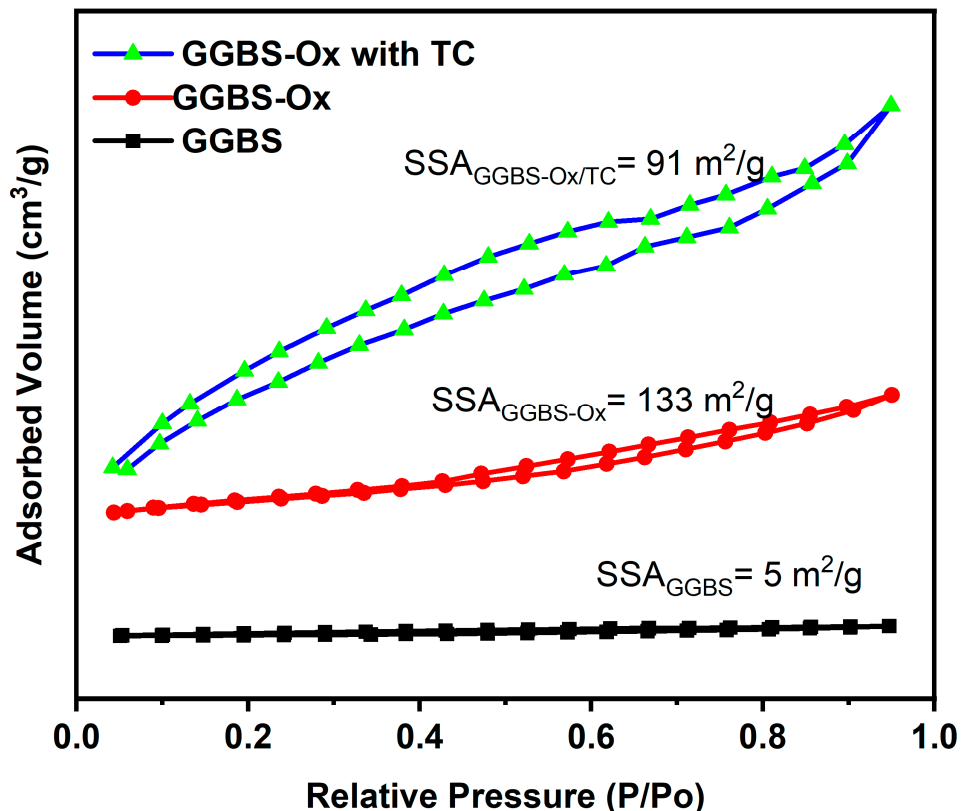


Figure. S2. N_2 adsorption and desorption isotherms of GGBS and GGBS-Ox

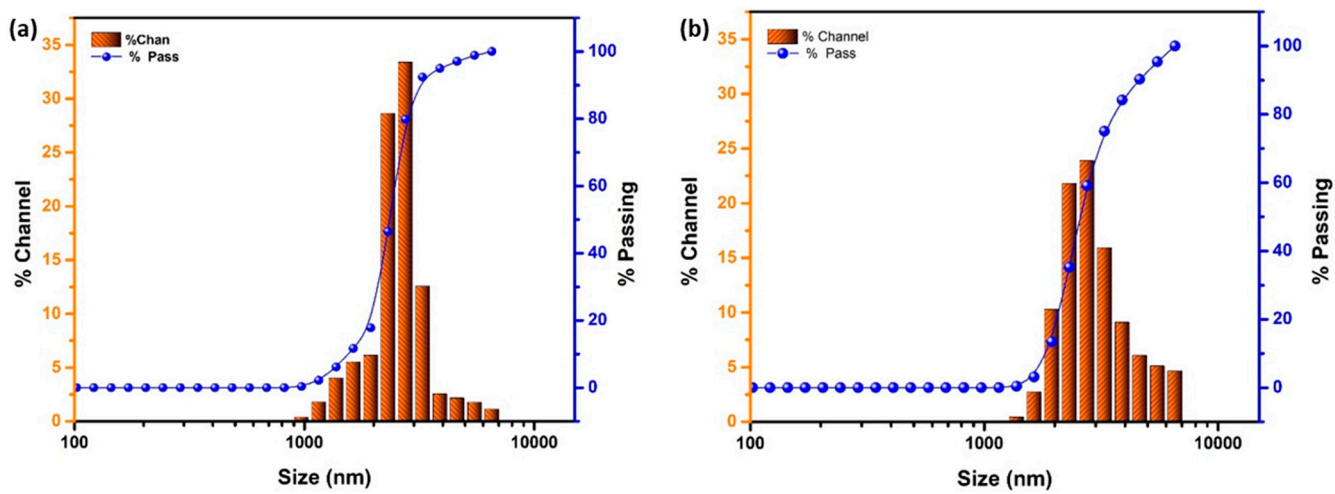


Figure. S3. (a) Particle size distribution by dynamic light scattering (DLS) of GGBS (b) Particle size distribution by dynamic light scattering (DLS) of GGBS-Ox

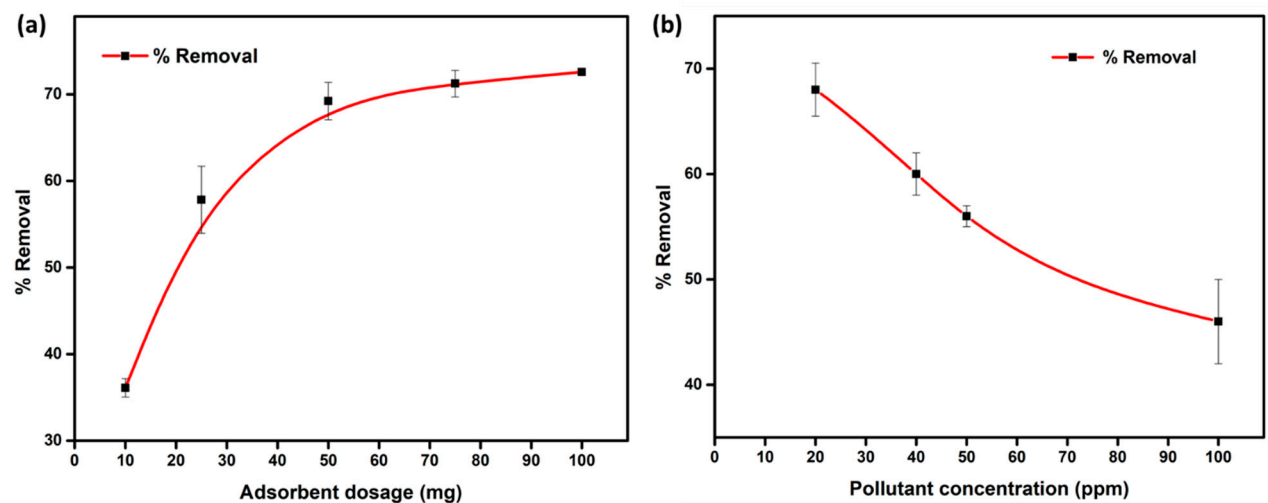


Figure. S4. (a)The effect of adsorbent dosage on percentage removal (b) the effect of pollutant concentration on the percentage removal.

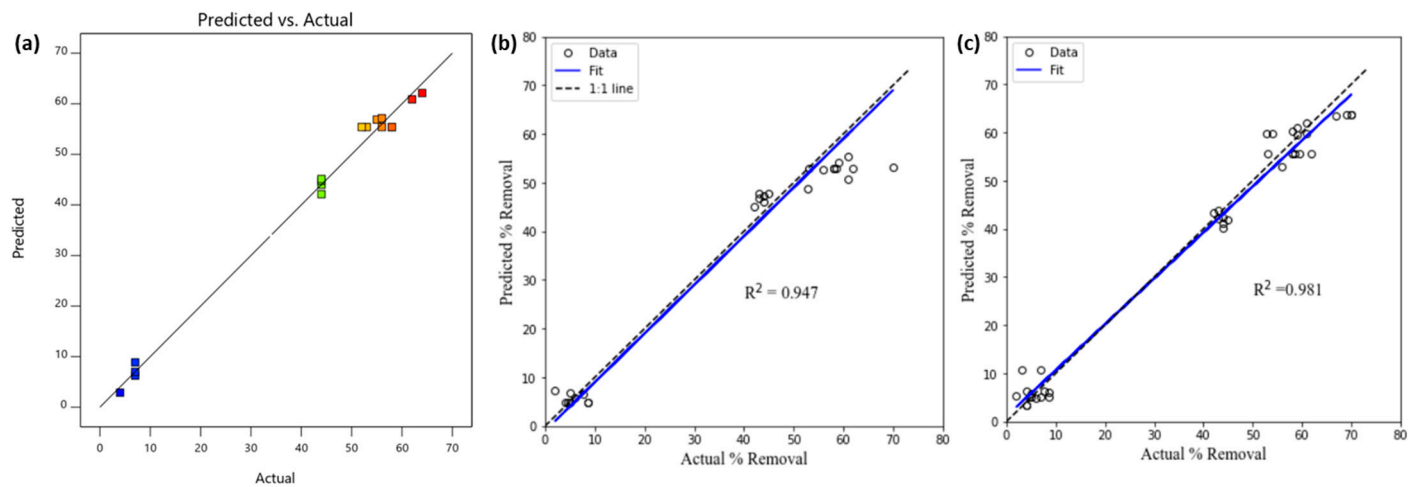


Figure. S5. (a) Comparison of predicted and actual results for RSM (b) Comparison of predicted and actual results for ANN (c) Comparison of predicted and actual results for RF

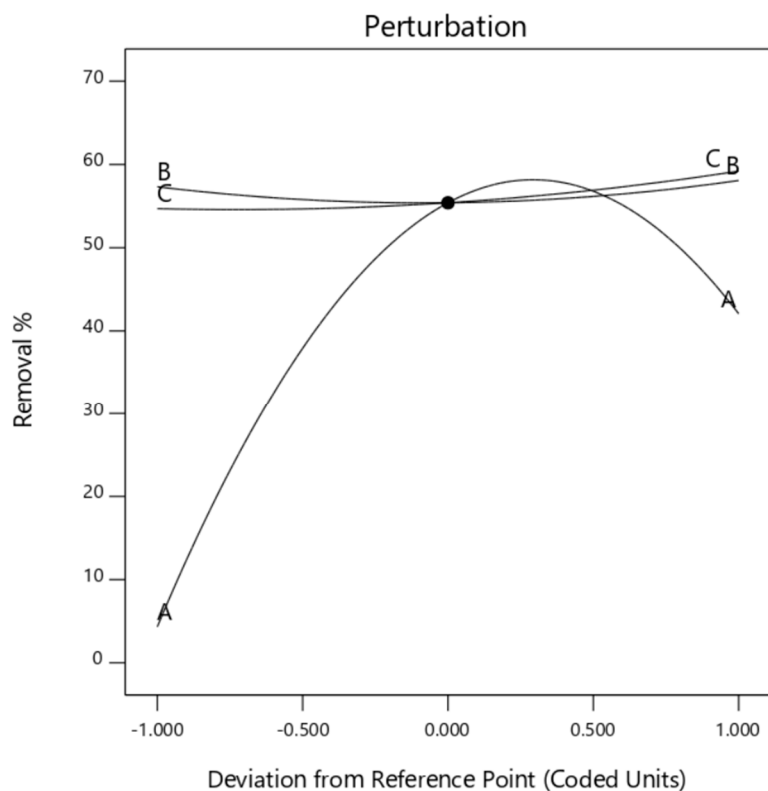


Fig. S6. Perturbation plot for TC removal efficiency.

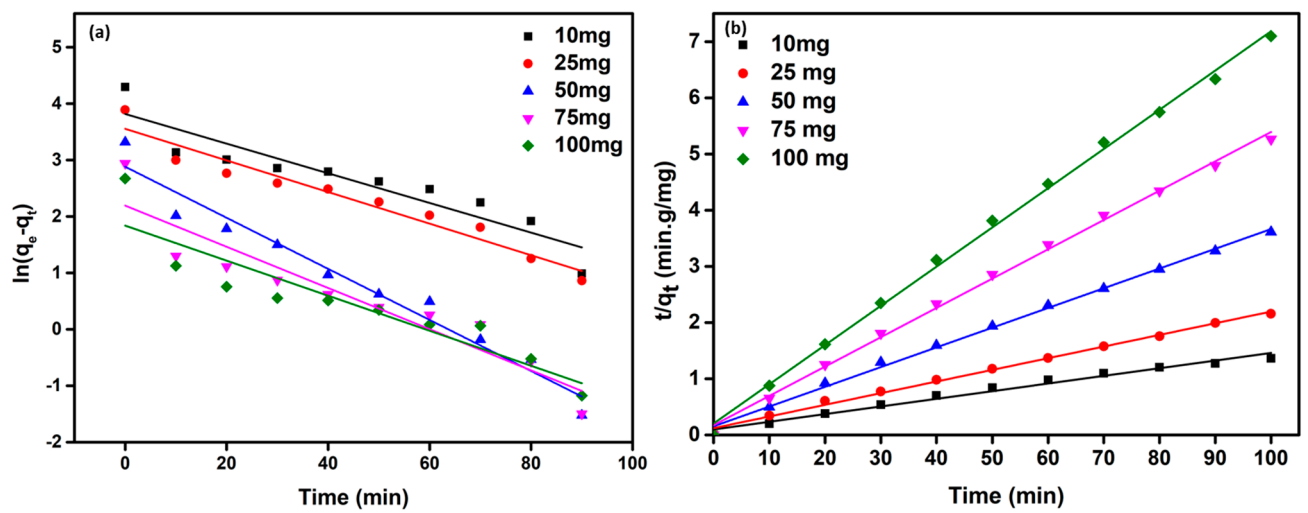


Figure S7. Kinetics of adsorption of TC ($C_0 = 40$ ppm, 50ml) (a) First-order kinetics (b) Second-order kinetics.

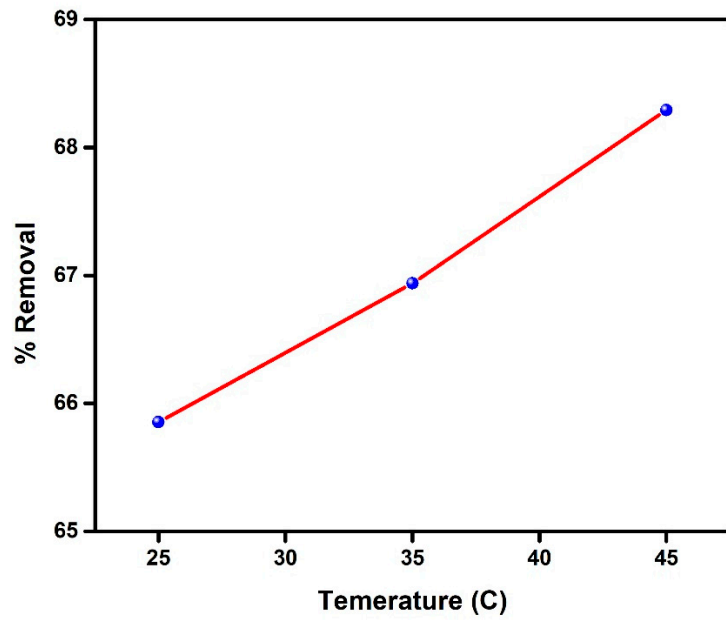


Figure. S8. Effect of the temperature on the adsorption capacity of TC by GGBS-Ox.

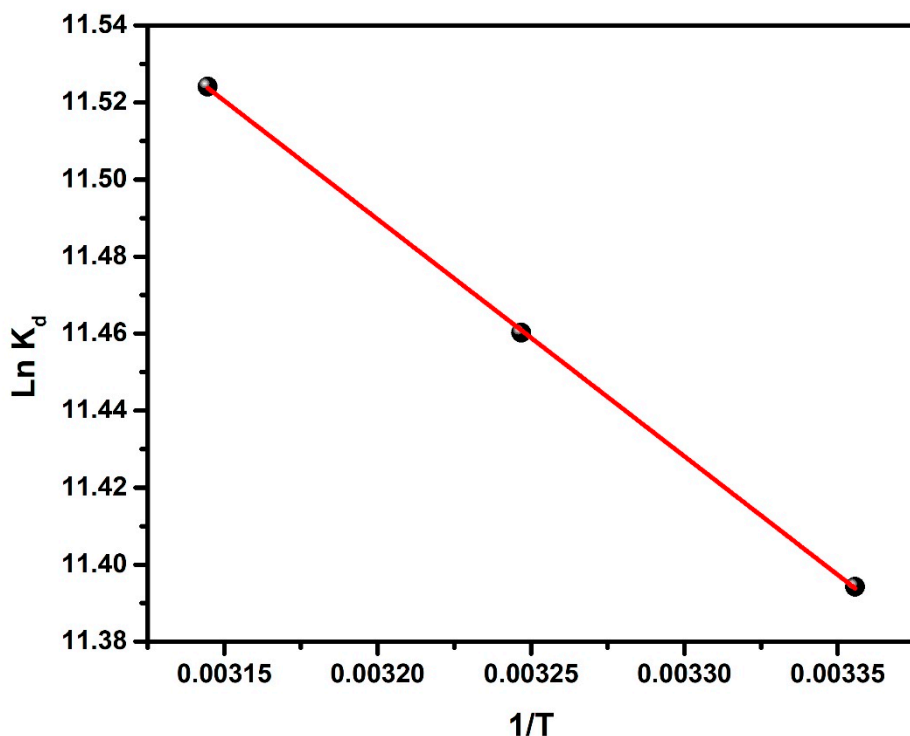


Figure S9. Thermodynamic parameters of TC adsorption by GGBS-Ox.

Table S1

Levels of parameters for BBD experiments.

Independent parameters	Coded and uncoded values		
	-1	0	+1
Initial pH	2	7	12
Contact time (min)	10	50	90
Stirring speed (rpm)	100	300	500

Table S2

Comparison of RSM, ANN, and RF

Parameter			
Model	R ²	RMSE	MAE
BBD	0.98	1.78	1.53
ANN	0.95	5.46	4.12
RF	0.98	3.43	2.81

Table S3. Calculation of adsorption parameters and regression coefficients

Kinetic model	Initial concentration (ppm)	Parameter	Regression coefficient
Pseudo-first order	q _e	K ₁	R ²
	20	15.95	0.027±0.002
	50	33.08	0.031±0.002

	100	53.60	0.022±0.003	0.8015
Pseudo-second order		q_e	K_2	R^2
	20	15.50	0.0621±0.001	0.9973
	50	32.19	0.0298±0.001	0.9959
	100	50.00	0.019±0.001	0.9955
Intraparticle		C_i	K_{id}	R^2
diffusion	20 (step 1)	12.17±0.155	0.34 ± 0.017	0.9842
	20 (step 2)	5.35±0.79	1.96± 0.22	0.9623
	50 (step 1)	9.55±1.76	4.20±0.5	0.9588
	50 (step 2)	23.57±1.19	0.93±0.13	0.8860
	100 (step 1)	7.99±1.08	8.33±0.30	0.9960
	100 (step 2)	33.92±1.88	1.87±0.21	0.9267

Table S4. The parameters and regression coefficients for pseudo-first order and pseudo-second order are listed below.

Kinetic model	Adsorbent dosage (mg)	Parameter	Regression coefficient
Pseudo-first order		q_e	K_1
	10	73.40	0.026±0.003
	25	49	0.028±0.002
	50	27.70	0.045±0.003
	75	19.00	0.036±0.004
	100	14.51	0.031±0.004
Pseudo-second order		q_e	K_2
	10	73.40	0.0136
	25	49	0.0200
			0.9944

50	27.70	0.0371	0.9964
75	19.00	0.0530	0.9968
100	14.51	0.0680	0.9974

Table S5. The parameters and regression coefficients for Langmuir, Freundlich, DR isotherm and McKay external diffusion model

Isotherm model	Parameters	Regression coefficient	
Langmuir	$q_m: 76.3942$	$k_L: 0.0452$	0.9820
Freundlich	$n: 1.76$	$k_F: 6.18$	0.9312
DR	$B : 7.53 \times 10^{-6}$	$E: 257 \text{ kJ/mol}$	0.8601
			Concentration Diffusion coefficient, $\text{cm}^2/\text{s} (\beta)$
McKay	20	3.812×10^{-9}	0.97
	50	2.310×10^{-9}	0.84
	100	1.564×10^{-9}	0.84

Table S6. Thermodynamic conditions for GGBS-Ox adsorption at different temperatures.

Temperature (K)	1/T	lnK _d	ΔG° (kJ/mol)	ΔH° (kJ/mol)	ΔS° (kJ/mol.K)	R ²
298	0.003356	11.3942	-28.2299			
308	0.003247	11.4602	-29.3462	5.1169	0.1119	0.9998
318	0.003145	11.5241	-30.4680			